INTERNATIONAL JOURNAL OF REFRIGERATION 38 (2014) 58–70

Available online at www.sciencedirect.com

ScienceDirect

journal homepage: www.elsevier.com/locate/ijrefrig

NLP model-based optimal design of LiBr–H_2O absorption refrigeration systems

María S. Mazzei [a], *Miguel C. Mussati* [a,b], *Sergio F. Mussati* [a,b,*]

[a] *CAIMI Centro de Aplicaciones Informáticas y Modelado en Ingeniería (UTN-FRRo), Zeballos 1341, S2000BQA, Rosario, Argentina*

[b] *INGAR Instituto de Desarrollo y Diseño (CONICET-UTN), Avellaneda 3657, S3002GJC, Santa Fé, Argentina*

ARTICLE INFO

Article history:
Received 3 March 2013
Received in revised form
24 October 2013
Accepted 27 October 2013
Available online 6 November 2013

Keywords:
LiBr–H_2O absorption refrigeration systems
Optimal design
Mathematical programming

ABSTRACT

This paper addresses the optimization of a single effect absorption refrigeration system operating with lithium bromide-water solution. A non-linear programming mathematical model is developed to determine the operating conditions and the distribution of the total heat transfer area (sizes) along the involved process units to optimize the following two objective functions: (i) maximization of the coefficient of performance for a given amount of the total heat transfer area, and (ii) minimization of the total heat transfer area of the system for a given cooling capacity. The proposed model can either be used for simulation or optimization purposes. Simulated or optimized values of temperature, pressure, composition and flow rate of all streams and sizing of each process unit are predicted. In addition, because of the non linear nature of the resulting model, a systematic solution procedure is proposed in order to guarantee the model convergence. A detailed discussion of the optimization results are presented through different case studies.

Conception optimale basée sur un modèle PNL (Programmation Non Linéaire) pour des systèmes frigorifiques à absorption de LiBr-H_2O

Mots clés : Systèmes frigorifique à absorption de LiBr-H_2O ; Conception optimale ; Programmation mathématique

* *Corresponding author*. INGAR Instituto de Desarrollo y Diseño (CONICET-UTN), Avellaneda 3657, S3002GJC, Santa Fé, Argentina. Tel.: +54 342 4534451; fax: +54 342 4553439.

E-mail addresses: solmazzei@hotmail.com (M.S. Mazzei), mmussati@santafe-conicet.gov.ar (M.C. Mussati), mmussati@santafe-conicet.gov.ar (S.F. Mussati).

0140-7007/$ – see front matter © 2013 Elsevier Ltd and IIR. All rights reserved.
http://dx.doi.org/10.1016/j.ijrefrig.2013.10.012

Nomenclature

A	Heat transfer area (m^2)
AMPL	A mathematical programming language
ARSs	Absorption refrigeration systems
COP	Coefficient of performance
F	Flow rate ($kg\ s^{-1}$)
GAMS	General algebraic modeling system
gPROMS	general PROcess Modeling System
H	Enthalpy ($kJ\ kg^{-1}$)
LCA	Life cycle assessment
LMTD	Logarithmic mean temperature difference (°C)
LP	Linear programming
MVCRSs	Mechanical vapor compression refrigeration systems
OP1	Optimization problem 1
OP2	Optimization problem 2
MILP	Mixed integer linear
MINLP	Mixed integer non linear programming
NLP	Non linear programming
P_THTA	Parameter related to the total heat transfer area
P	Pressure (kPa)
Q	Heat ($kJ\ s^{-1}$)
T	Temperature (°C)
THTA	Total heat transfer area (m^2)
U	Heat transfer coefficient ($kW\ m^{-2}\ °C^{-1}$)
X	Composition (%)
ΔT	Temperature difference (°C)

Subscripts and superscripts.

ABS	Absorber
CW	Cooling water
COND	Condenser
EV1	Expansion valve 1
EV2	Expansion valve 2
EVAP	Evaporator
GEN	Generator
hw	Hot water
in	Inlet
out	Outlet
R	Refrigerant
SHE	Solution heat exchanger
Sat_V	Saturated vapor
Sat_L	Saturated liquid water
SS	Strong solution
WS	Weak solution
1…11	Numbering system used to denote state point in Fig. 1.

1. Introduction

In recent years, special attention has been paid to the absorption refrigeration systems (ARSs) because of their environmentally friendly operation and low total cost. In comparison to the conventional mechanical vapor compression refrigeration systems (MVCRSs), ARSs require lower energy level, therefore renewable energy sources or heat wasted by industrial processes can be used to operate such systems and lead to cut global CO_2 emissions and reduce the global warming problem.

Several system-specific computer models have been developed that have proved to be very valuable tools for both research and development and design optimization (Grossman et al., 1979, Grossman 1982, 1998, Grossman and Childs 1983, McLinden and Klein 1985, Perez-Blanco and Patterson 1986, Vliet et al., 1982). Details on how each process unit of single and double-effect LiBr-water chillers are modeled and implemented in ABSIM, a user-oriented computer code designed for the simulation of absorption systems at steady state, can be found in Grossman (1998).

Different methodologies have been proposed and applied to accomplish the challenge of improving ARSs. Certainly, many works dealing with the study of ARSs based on energy analysis (pinch analysis), exergy analysis, thermoeconomics, and mathematical programming have been published. The major advantages of the pinch analysis is that the main trade-offs existing among energy (quality and quantity), driving forces, and required heat transfer areas can be represented in simple diagrams (e.g. grand composite curves GCC); thus, heat loads and shaftwork targets for the system under consideration can be readily estimated prior to design (Feng and Zhu, 1997). Exergy analysis is widely applied in a systematic way to evaluate the thermal efficiency level of a system, and to identify the most inefficient system components. Special attention should then be focused on such a component to minimize its irreversible losses. Exergy analysis is being applied to the analysis of different chemical plants, such as steel production, pulp and paper, oil processes, heat pumps, vapor recompression systems, residual gases treatment systems, biological processes, steam turbine systems, combustion processes, and thermal processes design. In some cases, the exergy analysis can better and more accurately assess the location of inefficiencies than the energy analysis. Kaynakli and Yamankaradeniz (2007) studied the performance of $LiBr–H_2O$ ARSs evaluating the entropy generation of the individual components and the whole system by varying some design parameters through a computational model. Sencan et al. (2005) and Arora and Kaushik (2009) developed a simulation program to determine the operating conditions that increase both the coefficient of performance (COP) and the total exergetic efficiency of a single effect $LiBr–H_2O$ system. Morosuk and Tsatsaronis (2008) performed an exergy analysis in a more advanced way, which consists of splitting the exergy destruction into the ARSs components, and then identifying the potential for improvement in each one. Thermoeconomics has provided an alternative and useful tool for the improvements of thermal systems. Indeed, several authors studied the application of thermoeconomic theory to the economic optimization of $LiBr–H_2O$ ARSs and conventional refrigeration plants, aimed at minimizing their operating costs and investments (Kodal et al., 2000; Kodal et al., 2002; Kodal et al., 2003; Misra et al., 2003, 2005, 2006; Sahin and Kodal, 2002; Palacios Bereche et al., 2009; Varani et al., 2003; Sahoo et al., 2005; Al-Otaibi et al., 2004; Kızılkan et al., 2007).

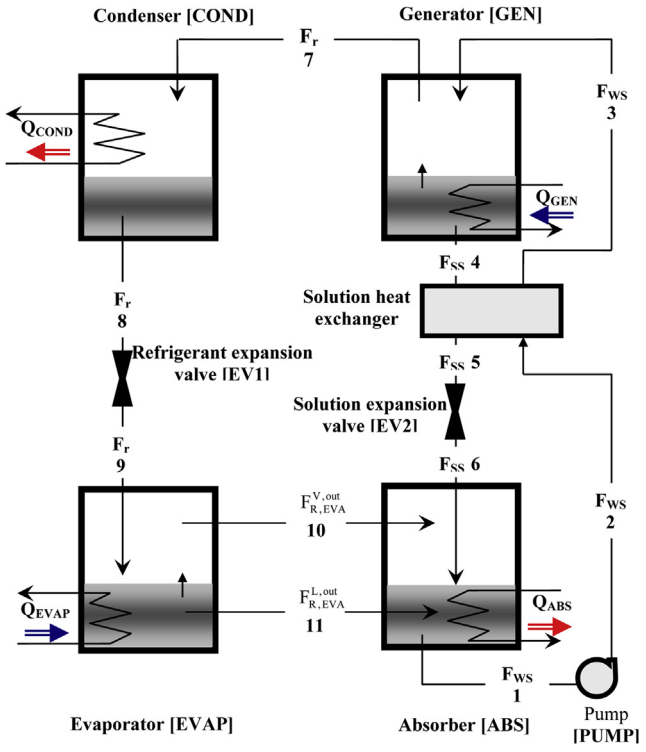

Fig. 1 – Diagram of a single effect LiBr–H_2O absorption refrigeration system.

Exergoeconomics is another widely used thermoeconomic approach, which combines exergetic and economic analyses. It determines intermediate product costs, heat transfer areas with the highest economic losses, and identifies the design and operation parameters to be analyzed and modified to achieve more efficient systems. Exergoeconomic analysis helps designers to improve the performance of a system in a cost effective way (Godarzi et al., 2013).

Systematic methods based on mathematical programming techniques have also been applied to the optimization of processes. Certainly, there has been a renewed interest in recent years for standard techniques such as linear (LP), non linear (NLP), mixed integer linear (MILP) and mixed integer non linear programming (MINLP) problems, especially when the optimization problem is combinatorial in nature (discrete decisions), of large size (number of equations and variables), and highly non linear. In fact, the performance of solvers handling non linear constraints was largely improved. In addition, disjunctive models as well as simulated annealing and genetic algorithm approaches are also efficiently used for optimization problems involving discrete and continuous variables. Mathematical programming environments such as GAMS (Brooke et al., 1996), gPROMS (Barton and Pantelides, 1993), and AMPL (Fourer et al., 1990) have proven to be powerful software tools, especially for optimization of combinatorial and highly non linear large scale systems.

A detailed review on synthesis and design problems solved by using mathematical programming-based approaches in diverse research areas can be found in Grossmann (2002) and Biegler et al. (1997). In contrast to the previous methods, the main advantages of the mathematical programming technique is that it allows to simultaneously optimize all the trade-offs existing among the process variables. However, only few publications deal with mathematical programming approaches applied to the optimization of energy conversion systems [24–31] (Chávez-Islas and Heard, 2009, Chávez-Islas et al., 2009; Gebreslassie et al., 2009a, 2009b; Sayyaadi and Nejatolahi, 2011; Marcos et al., 2011; Gebreslassie et al., 2010; Castro et al., 2008) and even fewer ones to environmentally benign refrigeration systems.

Chávez-Islas et al. (2009) applied MINLP techniques for the optimization of a NH_3–H_2O absorption refrigeration system. They developed a model that includes discontinuous functions for capital costs of the main system components. The simultaneous optimization of six decision variables (the reflux ratio, the temperature approaches in the absorber, condenser, subcooler, reboiler, and the economizer effectiveness) was performed in order to minimize the total annualized cost. The proposed model was applied to two types of heat rejection media: cooling water and air. The obtained results indicated that the selection of the cooling medium is dependent on the required refrigeration level. In addition, the influence of the design variables on the objective function depends strongly on the heat rejection medium type (air or water) and the process requirements (refrigeration level).

Recently, Gebreslassie et al. (2009a) presented a quantitative decision-support tool for the optimal design of environmentally conscious absorption cycles. A multi-objective NLP formulation that simultaneously accounts for the minimization of cost and environmental impact at the design stage was developed. The latter criterion was quantified by the Eco-indicator 99 methodology (Goedkoop and Spriensma, 2000), which follows the principles of the life cycle assessment (LCA) methodology (Pieragostini et al., 2012). The design task is formulated as a bicriteria NLP problem, whose solution is defined by a set of Pareto points that represent the optimal trade-off between the considered economic and environmental concerns. Thus, the decision-maker can choose the best Pareto solution point according to given preferences and the applicable legislation.

In this work an equation-oriented optimization mathematical model of single effect absorption refrigeration system operating with lithium bromide-water solution is presented. The proposed model enables the user to simultaneously optimize both the operating conditions and the sizes of the involved process units. The major contribution of this work is that the trade-offs that exist among the operating conditions (concentrations, flow-rates, pressures, temperatures) and the sizing of each process unit (heat transfer areas) are simultaneously optimized. The resulting predictive and deterministic model is based on mass and energy balances and design constraints. Given an objective function to be optimized [coefficient of performance (max.) or total heat transfer area (min.)] and design specifications, the model is able to simultaneously predict the optimal temperature, flow rate and composition values for each process stream and the distribution of the total heat transfer area (size) of each process unit. One of the optimization problems consists of determining the operating conditions and how a given amount of heat transfer area should be optimally distributed along the

system in order to maximize COP. In addition, for a fixed refrigeration capacity, the model is also solved to determine the optimal operating conditions and size of each process unit in order to minimize the total heat transfer area.

Because of the presence of non linear model constraints, an efficient and simple solution strategy is also proposed to avoid convergence problems.

The software tool General Algebraic Modeling System GAMS (Brooke et al., 1996), which is a high-level algebraic modeling system for large scale optimization, is used for implementing and solving the resulting mathematical model. As it will be discussed later, the obtained results show that the proposed mathematical model and the solution strategy have proven to be useful for both simulation and optimization purposes.

The paper is outlined as follows. Section 2 briefly describes a single effect LiBr–H_2O absorption refrigeration system. Section 3 summarizes the main model assumptions and includes the mathematical models of the involved process units. Section 4 is devoted to the statement and formulation of the optimization problem. Section 5 presents and discusses the results obtained for the analyzed case studies. Finally, conclusions and future works are pointed out in Section 6.

2. Single effect LiBr–H_2O absorption refrigeration system: process description

A scheme of the studied LiBr–H_2O absorption refrigeration system is depicted in Fig. 1, where LiBr are H_2O are the absorbent and the refrigerant fluids, respectively. It consists of a generator [GEN], an absorber [ABS], a condenser [COND], an evaporator [EVAP], a pump [PUMP], expansion valves for the refrigerant [EV1] and the solution [EV2] and a solution heat exchanger [SHE].

In the GEN, the LiBr–H_2O solution is heated for vaporizing and separating the refrigerant fluid (H_2O) from the solution. The refrigerant vapor flows to the COND, where heat is rejected to cooling water as the refrigerant condenses. Then, the condensed liquid flows through EV1 to the EVAP, where refrigerant is evaporated to produce cooling effect. The refrigerant vapor is afterward directed to the ABS, where it is absorbed by the high concentration solution coming from GEN, and rejects heat to the cooling water. Finally, the low concentration solution is pumped through SHE to the GEN. The low and high concentration solutions exchange heat in SHE.

Two different working fluid mixtures are mainly used in the absorption systems: LiBr–H_2O or NH_3–H_2O. The LiBr–H_2O working fluid is well suitable for cooling applications above 0 °C, and shows in general a higher coefficient of performance (COP) than NH_3–H_2O. The latter can work at lower temperatures than 0 °C, and the heat dissipation temperature is not limited by crystallization.

3. Mathematical model and assumptions

The process model comprises basically mass and energy balances and design equations for each process unit, and correlations to estimate process streams enthalpy. The complete model including physical relations and model implementation details (inequality constraints) is presented as Supplementary material.

The following key assumptions are made to derive the mathematical model:

- Steady state operation.
- Negligible pressure drop and heat loss in process units.
- The pump work is neglected in the total energy balance since it only consumes a relatively small amount of energy compared to the total heat transferred in the process.
- The expansion valves are adiabatic.
- The refrigerant states leaving the condenser and evaporator are assumed to be saturated liquid and gas, respectively.
- The refrigerant vapor leaving the generator is assumed to be superheated.
- The weak solution leaves the absorber at saturated liquid at equilibrium.
- The strong solution leaving the generator is in equilibrium at its respective temperature and pressure.
- Dependence of thermodynamic properties of the LiBr–H_2O solution on temperature and composition, and of water and steam on temperature and pressure.

4. Optimization problems statement

Given the single effect refrigeration system shown in Fig. 1 and its mathematical model presented in Supplementary material, the following two optimization problems (hereafter called OP1 and OP2) have been proposed.

a) Problem OP1. To determine the optimal distribution of a given amount of total heat transfer area (THTA) and operating conditions aiming at maximizing the coefficient of performance (COP). OP1 can be mathematically expressed as follows:

$$\begin{aligned}&\text{Maximize COP}\\&\text{s.t.}:\\&\begin{cases} h_s(x) = 0, \forall s \\ g_t(x) \le 0, \forall t \\ \text{THTA} = \text{P\_THTA} \end{cases}\end{aligned}$$

where x is the model variables vector, $h_s(x)$ refers to equality constraints (mass and energy balances, correlations for computing physico-chemical properties and size of each process unit). As mentioned earlier, the main equality constraints are presented in the Supplementary material [eq. (SM.1)–(SM.97)]. Inequality constraints are denoted by $g_t(x)$ and they are used, for instance, to avoid temperature cross situations and impose lower and upper bounds on some critical operating variables. The main inequality constraints are presented in Appendix B. THTA refers to the total heat transfer area and is computed by the sum of the heat transfer area of all process units. P_THTA is a model parameter which is related to THTA and it is varied in a wide range.

The problem consists of determining the optimal allocation of THTA in the system components, pressures, temperatures, flow-rates and compositions of streams in order to maximize the COP. Thus, for each values of P_THTA the COP is

Table 1 – Process data used for problems OP1 and OP2.

Parameter	Value
Temperature [ºC]	
Inlet temperature of the cooling water in the condenser [$T^{in,cw}_{COND}$]	27
Inlet temperature of the cooling water in the absorber [$T^{in,cw}_{ABS}$]	30
Inlet temperature of the chilled water in the evaporator [$T^{in,chilled\ water}_{EVAP}$]	13
Inlet temperature of the hot water in the generator [$T^{in,hw}_{GEN}$]	92
Heat transfer coefficient [kW m^{-2} ºC^{-1}]	
Evaporator [U_{EVAP}]	1.5[a]
Absorber [U_{ABS}]	0.7[a]
Condenser [U_{COND}]	2.5[a]
Generator [U_{GEN}]	1.5[a]
Solution heat exchanger [U_{SHE}]	1.0[a]

[a] Data taken from Gebreslassie et al. (2012).

maximized. The advantage of the model implementation and the advanced modeling tool used to solve the problem is that all decision variables are optimized simultaneously.

b) Problem OP2. To determine the optimal operating conditions aiming at minimizing the THTA for a given cooling capacity (Q_{EVAP}). OP2 can be formulated as follows:

$$\text{Minimize THTA}$$
$$\text{s.t.}: \begin{cases} h_s(x) = 0, \forall s \\ g_t(x) \le 0, \forall t \\ \text{Cooling capacity}(Q_{EVAP}) = 50\ \text{kW} \end{cases}$$

For both problems, OP1 and OP2, $h_s(x)$ and $g_t(x)$ are the same. Note that in OP1, Q_{EVAP} is a decision variable i.e. a free variable whose value results from optimization whereas THTA is set by the user. Precisely, the parameter P_THTA is varied from 1 to 55 m^2. In problem OP2, THTA is a decision variable whereas Q_{EVAP} is a model parameter (50 kW).

The parameters used for optimization are listed in Table 1.

The main decision variables considered for optimization are the temperature, pressure, composition and flow-rate of all streams. Lower and upper bounds of the main process variables set by the user are listed in Table 2. The lower and upper bounds for the temperatures of the refrigerant and LiBr solutions along the system components depend on the values of parameters listed in Table 1 and are imposed through the inequality constraints $g_t(x)$ presented in Appendix B. For instance, the lower bound used for the temperature of refrigerant leaving the condenser [T_8] is expressed in terms of the inlet temperature of the cooling water [$T^{in,cw}_{COND}$], as shown in eq. (B1).

Table 2 – Lower and upper bounds used for optimization.

Variable	Lower bound	Upper bound
LiBr concentration [%]	40	70
Pressure [kPa]	0.1	15
Mass flow-rate of refrigerant and LiBr solutions [kg s^{-1}]	0	100

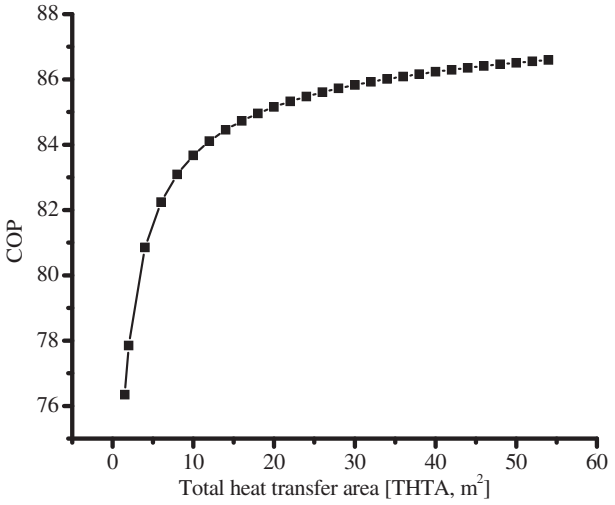

Fig. 2 – Coefficient performance vs. total heat transfer area.

5. Results and discussion

The correctness of the implementation and coding of the process mathematical model was first verified by comparing the obtained output results with those reported by Florides et al. (2003). A complete comparison of results is presented in Appendix C. Once the model was successfully verified, it was used to solve the two optimization problems stated in the previous section.

5.1. *Maximization of COP for fixed total heat transfer areas (optimization problem OP1)*

This section discusses the optimal solutions obtained for the problem OP1. The optimal values of the COP, operating variables, distribution of the THTA, heat loads and log mean temperature differences (LMTDs) related to the heat transfers are shown in terms of the THTA in separate figures, from Figs. 2 to 9. Each one of the values illustrated in these figures

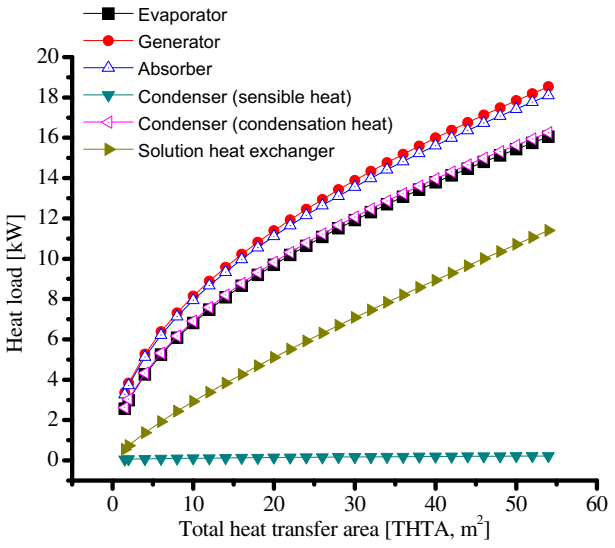

Fig. 3 – Heat load vs. total heat transfer area.

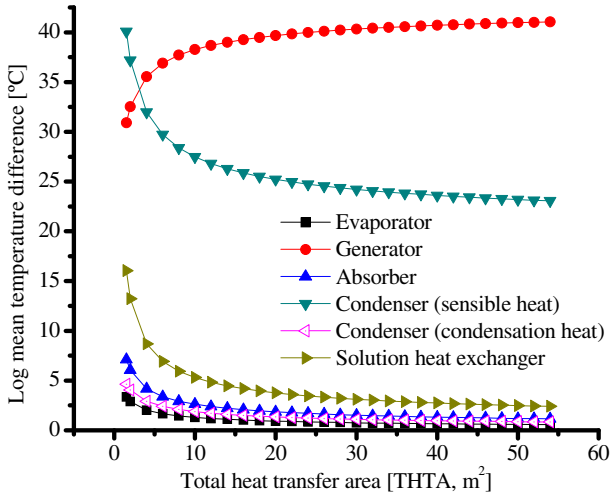

Fig. 4 – Log mean temperature difference vs. total heat transfer area.

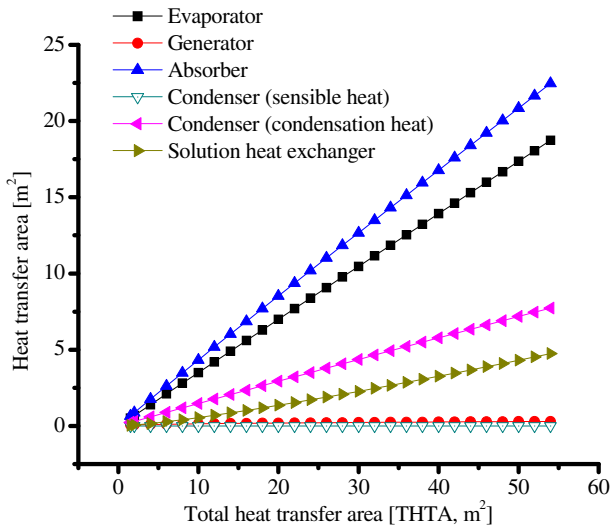

Fig. 5 – Heat transfer area vs. total heat transfer area.

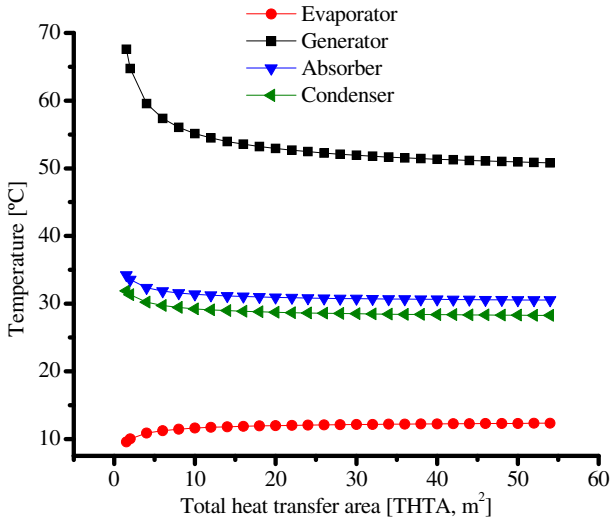

Fig. 6 – Temperature vs. total heat transfer area.

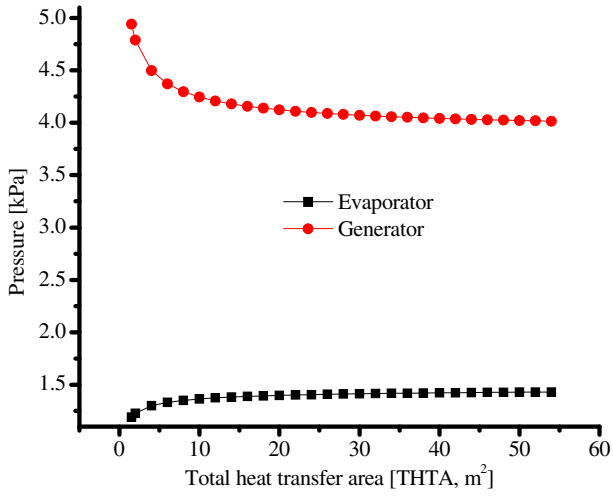

Fig. 7 – Pressure in the evaporator and generator vs. total heat transfer area.

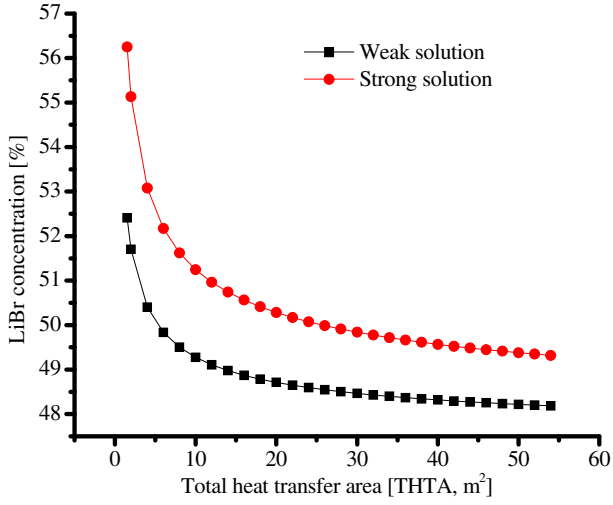

Fig. 8 – Libr concentration of the weak and strong solutions vs. total heat transfer area.

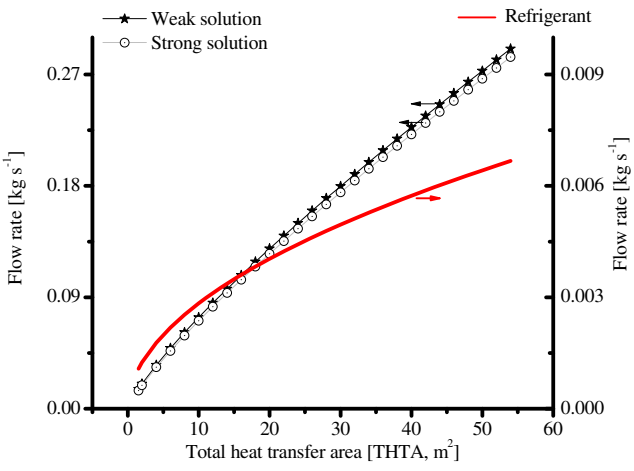

Fig. 9 – Flow rate of refrigeration, weak and strong solutions vs. total heat transfer area.

corresponds to optimal values. Therefore, the complete optimal solution for a given value of THTA can be directly derived from these figures.

Fig. 2 shows a significant increase of COP at lower values of THTA (from THTA = 1 to THTA = 15 m^2) because Q_{GEN} increases faster than Q_{EVAP} (Fig. 3). Then, from THTA = 15 m^2 the COP increases slowly. This behavior can be explained taking into account the different trade-offs existing between the LMTDs and heat loads in each heat exchanger which play an important role in the distribution of the total heat transfer area. The heat loads in all pieces of equipment can increase by increasing the heat transfer area and/or by increasing the LMTD for the heat transfer. It should be mentioned that despite the THTA is fixed, its distribution along the heat transfer units and temperatures and thereby LMTDs are the main decision variables of the problem.

Specifically, Figs. 3–5 show that, in the generator, Q_{GEN} increases by the increase of both A_{GEN} and $LMTD_{GEN}$, whereas in the evaporator, Q_{EVAP} increases only by the increase of A_{GEN} because $LMTD_{GEN}$ decreases as THTA increases. Optimal solutions reveal that the THTA is distributed more in the EVAP and ABS than in the GEN, COND and SHE (Fig. 5). Thus, the main differences between EVAP and GEN are in the trends of their driving forces and magnitudes. The higher THTA, the higher $LMTD_{GEN}$ and the lower $LMTD_{EVAP,}$ resulting in a better distribution of THTA in order to maximize the COP. The corresponding optimal values of pressure, temperature, flow-rate and composition of all streams (weak and strong solutions and refrigerant) that lead to the maximum values of COP are shown from Figs. 6 to 9.

As shown in Fig. 8, the lower THTA the higher concentration differences. Fig. 9 shows how the flow-rate of refrigerant and LiBr solutions increase with the increase of THTA.

5.2. *Minimization of THTA for a fixed cooling capacity (50 kW)*

For same model parameters listed in Tables 1 and 2, the model was also used to solve the problem OP2, that is, the minimization of the total heat transfer area for a given cooling capacity (50 kW). Once again, it is important to mention that the optimal trade-offs among the distribution of THTA, heat loads, LMTDs, flow-rates and compositions are optimized simultaneously.

Tables 3 and 4 list the optimal values obtained.

As shown in Table 4 the minimum THTA required by the whole process is 23.86 m^2 and the corresponding value of COP is 75.54.

Finally, the model was solved in order to show how the optimal solutions vary when the THTA is increased from the minimum value (23.86 m^2) for the same cooling capacity (50 kW). Thus, the only difference compared to the optimization problem solved in Section 5.1, is that Q_{EVAP} is now fixed (50 kW). Thus, the optimal distribution of THTA along the system component and operating conditions are determined in order to maximize COP. It should be noted that, because Q_{EVAP} is fixed, the maximization of COP is equivalent to minimize Q_{GEN}. The obtained results are presented from Figs. 10 to 14.

Table 3 – Optimal values for cooling capacity = 50 kW.

	F (kg s^{-1})	T (°C)	P (kPa)	X (%)
1	$165.39 \cdot 10^{-4}$	37.7	1.004	55.88
2	$165.39 \cdot 10^{-4}$	37.7	4.984	55.88
3	$165.39 \cdot 10^{-4}$	54.7	4.984	55.88
4	$144.38 \cdot 10^{-4}$	84.8	4.984	64.02
5	$144.38 \cdot 10^{-4}$	62.8	4.984	64.02
6	$144.38 \cdot 10^{-4}$	53.9	1.004	64.02
	$\varphi = 0.007$			
7	$21.01 \cdot 10^{-4}$	84.8	4.984	0
8	$21.01 \cdot 10^{-4}$	32.1	4.984	0
9	$21.01 \cdot 10^{-4}$	7.0	1.004	0
	$\varphi = 0.043$			
10	$21.01 \cdot 10^{-4}$	7.0	1.004	0
11	0[a]	7.0	1.004	0

φ = steam quality.
[a] It is zero because the stream leaving the evaporator is saturated vapor.

Table 4 – Optimal distribution of the total heat transfer area and heat loads.

Unit	Heat load	Heat transfer area [m^2]
Evaporator	50.00[a]	4.61
Absorber	63.73	8.12
Generator	66.18	6.95
Condenser	52.45	3.14
Solution heat exchanger	5.77	1.04

[a] Fixed value.

As expected, Fig. 10 shows that COP increases as THTA increases.

From Fig. 12 it can be seen that the trends of the LMTD in each one of the system units and thereby temperatures are similar to those obtained previously (Fig. 4). However, the trends of heat loads, heat transfer areas and flow-rates observed in Figs. 11, 13 and 14 (OP2) differ from those presented in Figs. 3, 5 and 9 (OP1). Certainly, for a fixed $Q_{EVAP,}$ both Q_{GEN} and A_{GEN} decrease with the increase of THTA. This can be explained as follows. As mentioned earlier, the maximization

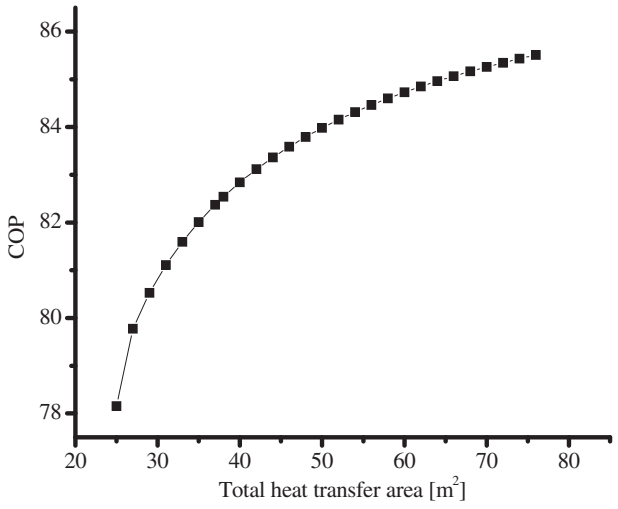

Fig. 10 – Coefficient performance vs. total heat transfer area (cooling capacity of 50 kW).

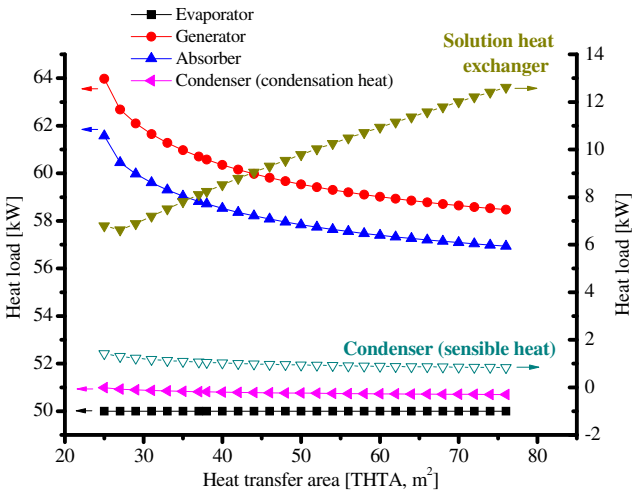

Fig. 11 – Heat load vs. total heat transfer area (cooling capacity of 50 kW).

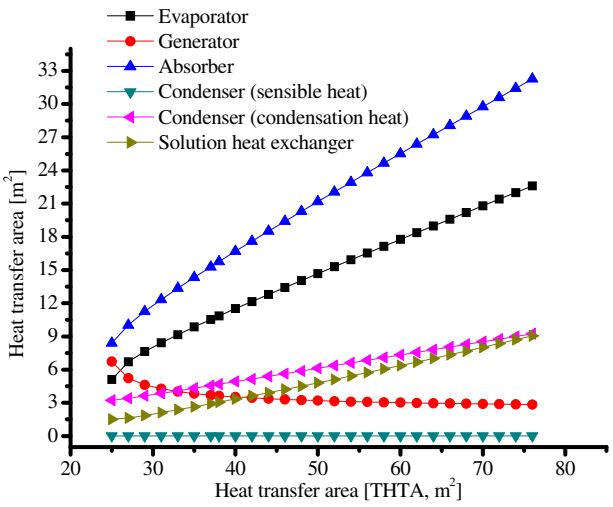

Fig. 13 – Heat transfer area vs. total heat transfer area (cooling capacity of 50 kW).

of COP implies the minimization of Q_{GEN} for which it is necessary to decrease A_{GEN}. Therefore, less amount of A_{GEN} is distributed in the generator with the increase of THTA as shown in Fig. 13.

It is interesting to observe the trade-offs among THTA, Q_{ABS}, A_{ABS} and $LMTD_{ABS}$. Results in Figs. 11–13 show that A_{ABS} increases as THTA increases but Q_{ABS}. however, decreases as THTA increases. This is caused by the decreasing of $LMTD_{ABS}$.

Finally, it should be mentioned that the optimal trends of LiBr concentrations and pressures of refrigerant, weak and strong solution streams are similar to those obtained in the previous optimization study but with different numerical values (results not presented in this work). However, the refrigerant flow rate decreases with the increase of THTA (Fig. 14), in contrast to what was observed for OP1 (Fig. 9).

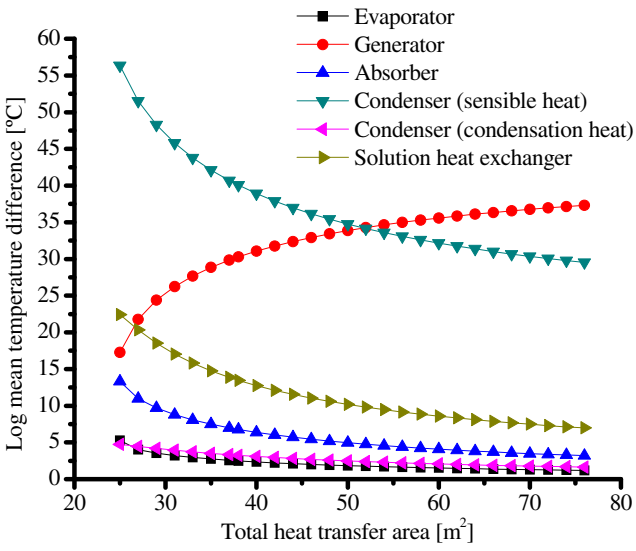

Fig. 12 – Log mean temperature difference vs. total heat transfer area (cooling capacity of 50 kW).

6. Computational implementation aspects and solution strategy

The resulting NLP model involves about 150 equality and 150 inequality constraints. It was implemented in General Algebraic Modeling System GAMS (Brooke et al., 1996), which is an oriented-to-equations modeling environment and is flexible enough to allow users to define different models and implement the solution strategy. A local NLP solver code CONOPT 2.041 was used (Drud, 1992), which is based on the generalized reduced gradient algorithm. As such, global optimal solutions cannot be guaranteed.

As mentioned earlier, the model involves non linear and non convex constraints arising mainly from logarithms and bilinear terms (multiplication of two or more variables), which can lead to local optimal solutions and/or convergence problems. Therefore, an efficient strategy for variables initialization is then essential for the model convergence. Different initialization and solution strategies can be used in order to address non convex NLP problems (Biegler et al., 1997; Ryoo and Sahinidis, 1995;

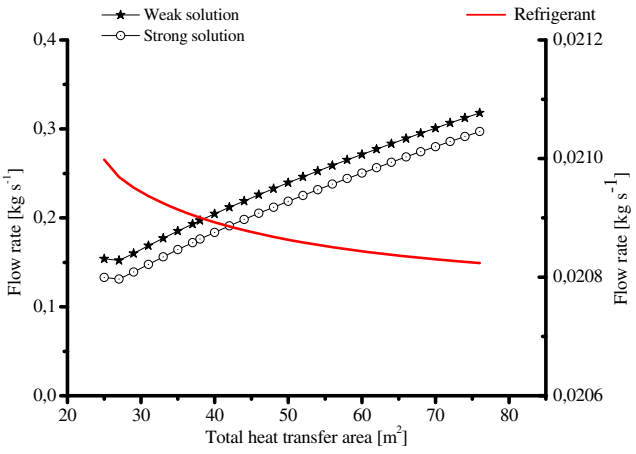

Fig. 14 – Flow rate of refrigeration, weak and strong solutions vs. total heat transfer area cooling capacity of 50 kW).

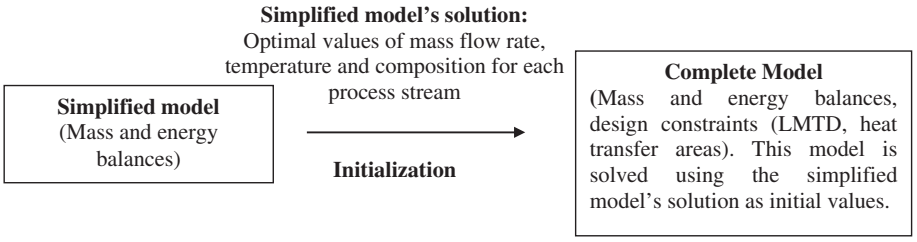

Fig. 15 – Efficient solution strategy.

Floudas, 2000). A simple and efficient methodology was here applied, which is schematized in Fig. 15. The methodology consists on starting the optimization of the complete model from a feasible solution in order to get convergence in a few iterations. For doing so, two different models involving different complexity or detail degree are solved, which are referred as the simplified model and the complete model (Fig. 15).

First, the simplified model, which considers only the mass and energy balances, is solved via simulation (constraints used to compute LMTD and heat transfer areas are not considered). This first solution provides composition, temperature and flow rate values for all process streams, which are, in fact, a feasible solution for the complete model. Then, the complete model, which includes the simplified model along with design constraints (constraints used to compute LMTD and heat transfer areas) is solved using the solution obtained from the simplified model as initial values. After that, for a given amount of total heat transfer area (THTA), the complete model is solved to maximize COP. Then, THTA is increased and the model is solved using the previous solution as starting point. This procedure is systematically repeated to cover the range of interest for THTA. The proposed initialization method guarantees the convergence of the model. The successive optimization problems, i.e. the steps of the solution strategy illustrated in Fig. 15, can be executed automatically with only one "optimize" command execution. Some variables and equations have been properly scaled in order to improve the convergence of the model.

Using the proposed solution strategy, the complete mathematical model converges in a few number of iterations and few seconds of CPU time. Certainly, each optimization problem requires approx. 95 iterations and 0.1 s.

Finally, model initialization based on random values has also been tried. It was observed that the convergence of the model strongly depends on the used initial values. For some random initial values sets, when the model has converged, the same optimal that is computed by using the strategy proposed in Fig. 15 was found, but for other random initial values sets convergence problems were observed. Then, it is easy to conclude that the solution strategy proposed in Fig. 15 is more effective than the use of initial random values.

7. Conclusions

This paper focused on developing a mathematical model of a single effect LiBr–H_2O refrigeration system to optimize the operating conditions and size of each system components in order to maximize COP. The model can be used for both simulation and optimization purposes. The coding of the proposed model in the GAMS environment has been successfully verified with data reported in the literature.

Then, the proposed model is solved to determine the optimal operating conditions and how a given total heat transfer area should be distributed along the system components in order to maximize COP.

The optimization problems only considered the following model parameters: inlet temperature of the cooling water in the condenser and absorber, inlet temperature of the chilled water and hot water in the evaporator and generator, and heat transfer coefficient in each system component. On the other hand, the pressure, temperature and flow-rate of each stream in each process component were the optimization variables. Thus, the trade-offs among heat loads, heat transfer areas and driving forces were optimized simultaneously. One of the obtained results reveal that the driving force in the generator increases as the total heat transfer area increases in contrast to that happen in the evaporator. These trends contribute to a better distribution of the total heat transfer area and heat loads along the process units to maximize the coefficient of performance. The optimal values of all process variables for a wide range of total heat transfer area were presented and discussed. Then, the optimization model was solved to find the minimum THTA for a fixed cooling capacity (50 kW).

A simple but efficient strategy to solve the proposed NLP model was presented and its features discussed. The solution methodology guarantees the model convergence when the model parameters (input data) are varied.

The proposed mathematical model will be further refined and extended to represent a double effect absorption refrigeration system. A hybrid methodology that combines the advantages of the mathematical programming approach and exergoeconomic analysis will be developed and applied to similar case studies.

Acknowledgment

The financial support from the Facultad Regional Rosario of the Universidad Tecnológica Nacional (FRRo) and the Consejo

Nacional de Investigaciones Científicas y Técnicas (CONICET) of Argentina are gratefully acknowledged.

Appendix A. Supplementary data

Supplementary data related to this article can be found at http://dx.doi.org/10.1016/j.ijrefrig.2013.10.012.

Appendix B

The following inequalities are included in order to avoid temperature crossovers. The subscripts "in" and "out" refer, respectively, the inlet and outlet while "cw" and "hw" refer to the cooling water and hot water.

$$T_8 \geq T_{COND}^{in,cw} + 0.1\,^{\circ}C \quad (B1)$$

$$T_7 \geq T_{COND}^{out,cw} + 0.1\,^{\circ}C \quad (B2)$$

$$T_{COND}^{out,cw} \geq T_{COND}^{in,cw} + 0.1\,^{\circ}C \quad (B3)$$

$$T_1 \geq T_{ABS}^{out,cw} + 0.1\,^{\circ}C \quad (B4)$$

$$T_{ABS}^{out,cw} \geq T_{ABS}^{in,cw} + 0.1\,^{\circ}C \quad (B5)$$

$$T_6 \geq T_{ABS}^{out,cw} + 0.1\,^{\circ}C \quad (B6)$$

$$T_{10} \leq T_{EVAP}^{out,chilledwater} + 0.2\,^{\circ}C \quad (B7)$$

$$T_9 \leq T_{EVAP}^{out,chilledwater} + 0.2\,^{\circ}C \quad (B8)$$

$$T_{EVAP}^{in,chilledwater} \leq T_{EVAP}^{out,chilledwater} + 0.2\,^{\circ}C \quad (B9)$$

$$T_4 \leq T_{GEN}^{in,hw} - 0.1\,^{\circ}C \quad (B10)$$

$$T_3 \leq T_{GEN}^{out,hw} - 0.1\,^{\circ}C \quad (B11)$$

Appendix C

Verification of model

As mentioned in Section 5, the proposed model verified by comparing the obtained output results with those reported by Florides et al. (2003). Only for comparison purpose, the model was used as a "simulator" rather than an "optimizer". For doing so, it was necessary to fix several optimization variables (i.e. degree of freedom) at the same values as reported by Florides et al. (2003). Table C1 lists the input data corresponding to the main model parameter values used for verification. Table C2 compares the predicted values of the thermodynamic properties and flow rates of all process streams, while Table C3 compares the heat loads in each piece of equipment involved in the cycle, and the overall cycle performance.

The comparisons of results listed in Tables C2 and C3 reveal a good agreement between the predicted and reported values.

Also, the verification of the model included the sensitivity analysis presented in Florides et al. (2003). More precisely, the authors studied influence of the absorber inlet LiBr concentration on the coefficient of performance, pump mass flow rate and absorber exit temperature. The absorber inlet LiBr concentration was varied from 45.0 to 57.5% and parameter values listed in Table C4 were assumed.

From the obtained simulation output results shown in Fig. C1, it can be clearly observed that the COP decreases as the absorber inlet LiBr concentration increases. Since the cooling capacity is kept constant at 10.0 kW, the higher absorber inlet LiBr concentrations, the lower heat requirements in the evaporator, and consequently, the lower COP values. In addition, the higher absorber inlet LiBr concentrations, the higher absorber exit temperatures and pump mass flow rates.

Finally, Fig. C2 shows the influence of the generator outlet temperature on the coefficient of performance, pump mass flow rate and absorber exit temperature. Table C5 lists the assumed design parameter values for this case. The outlet temperature of the solution at the generator [$T_{RV,GEN}^{out}$] has been varied from 65.0 to 115.0 °C. Fig. C2 plots the obtained simulation output results.

The obtained results show that by keeping constant Q_{EVAP}, T_3, T_{10}, T_1, P_1 and the absorber inlet LiBr concentration X_6 (Table C5), it can be observed from Fig. C2 that if the generator temperature (T_4 and T_7) increases, the generator pressure also increases, resulting in an enthalpy increase of the refrigerant and the solution leaving the generator, which thereby increases the generator load (Q_{GEN}). In addition, the heat removed in the condenser also increases. Thus, the value of COP (Q_{EVAP}/Q_{GEN}) decreases as the generator temperature increases.

In addition it should be mentioned that the simulated results also reveal that the pump mass flow is not significantly influenced by the generator outlet temperature. In addition it should be mentioned that the simulated results also reveal that the pump mass flow is not significantly influenced by the generator outlet temperature. Indeed, the pump mass flow varies slightly over the range of input generator outlet temperature values; it decreases from 0.04 kg s^{-1} at 65 °C to 0.037 kg s^{-1} at 115 °C (6.5%).

Table C1 – Main model parameter values used for comparison (Florides et al., 2003).

Parameter	Symbol	Value
Evaporator capacity	Q_{EVAP}	10
Evaporator temperature [°C]	$T_{R,EVAP}^{out}$	6
Outlet temperature of the solution at the generator [°C]	$T_{SS,GEN}^{out}$	90
Weak solution mass fraction [% LiBr]	$X_{WS,ABS}^{out}$	55
Strong solution mass fraction [% LiBr]	$X_{SS,GEN}^{out}$	60
Outlet temperature of the solution at the heat exchanger [°C]	$T_{WS,SHE}^{out}$	65
p	$F_{R,EVAP}^{out}$	$0.025 \cdot F_{R,EVAP}^{out}$

Table C2 – Comparison of thermodynamic properties and mass flow rate estimates for process streams.

Stream	h (kJ kg^{-1})		F (kg s^{-1})		P (kPa)		T (°C)	
	Florides et al.	This work	Florides et al.	This work	Florides et al.	This work	Florides et al.	This work
1	83.000	83.070	0.053	0.053	0.934	0.934	34.9	34.8
2	83.000	83.070	0.053	0.053	9.660	9.615	34.9	34.8
3	145.410	145.460	0.053	0.053	9.660	9.615	65.0	65
4	212.210	212.170	0.0486	0.0490	9.660	9.615	90.0	89.9
5	144.210	144.110	0.0486	0.0490	9.660	9.615	54.8	54.6
6	144.210	144.110	0.0486	0.0490	0.934	0.934	44.5	44.8
7	2628.052	2627.88	0.0044	0.0040	9.660	9.615	85.0	84.9
8	185.301	186.998	0.0044	0.0040	9.660	9.615	44.3	44.6
9	185.301	183.998	0.0044	0.0040	0.934	0.934	6.0	6.0
10	2511.802	2511.798	0.0043	0.0040	0.934	0.934	6.0	6.0
11	23.500	25.214	$1.10\cdot10^{-4}$	$1.07\cdot10^{-4}$	0.934	0.934	6.0	6.0

Table C3 – Energy flows involved in the main process components.

	Symbol	This work	Florides et al.
Evaporator capacity (kW)	Q_{EVAP}	10.00	10.00
Heat rejected from absorber to environment (kW)	Q_{ABS}	13.45	13.42
Heat input to the regenerator (kW)	Q_{GEN}	14.21	14.20
Heat rejected from condenser to environment (kW)	Q_{COND}	10.76	10.78
Coefficient of performance	COP	0.704	0.704
Effectiveness of SHE	E_L	0.523	0.524

Table C4 – Design parameter values assumed for verification of the model (Fig. B1).

Parameter	Value
Outlet temperature of the solution at the heat exchanger [°C]	55.0
Outlet temperature of the solution at the generator [°C]	75.0
Condenser temperature [°C]	70.0
Evaporator capacity	10.0
Evaporator temperature [°C]	6.0
Outlet LiBr percentage ratio at the absorber [%]	60.0
Generator and condenser pressure [kPa]	4.82
Absorber and evaporator pressure [kPa]	0.934
Absorber inlet LiBr concentration [%]	Varied from 45.0 to 57.5

Table C5 – Design parameters values assumed for verification of the model (Fig. B2).

Parameter	Value
Outlet temperature of the solution at the heat exchanger [°C]	55.0
Evaporator capacity	10.0
Evaporator temperature [°C]	6.0
Absorber inlet LiBr concentration [%]	52.5
Outlet temperature of the weak solution at the absorber [°C]	30.4
Absorber and evaporator pressure [kPa]	0.934
Generator exit temperature [°C]	Varied from 65 to 115

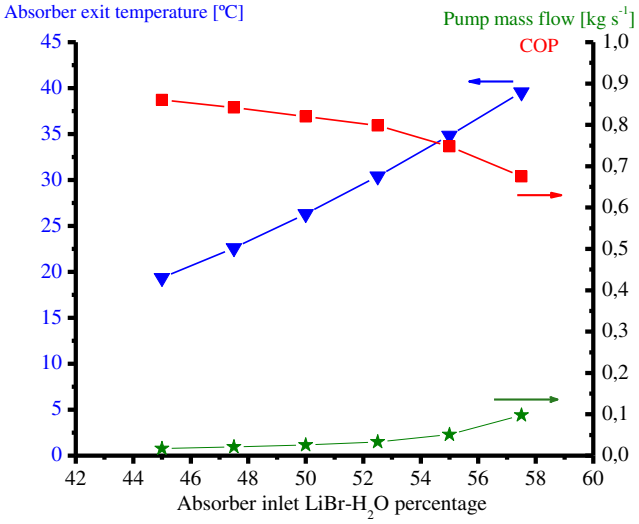

Fig. C1 – Influence of the absorber inlet LiBr concentration on the coefficient of performance, pump mass flow rate and absorber exit temperature (cooling capacity of 10 kW).

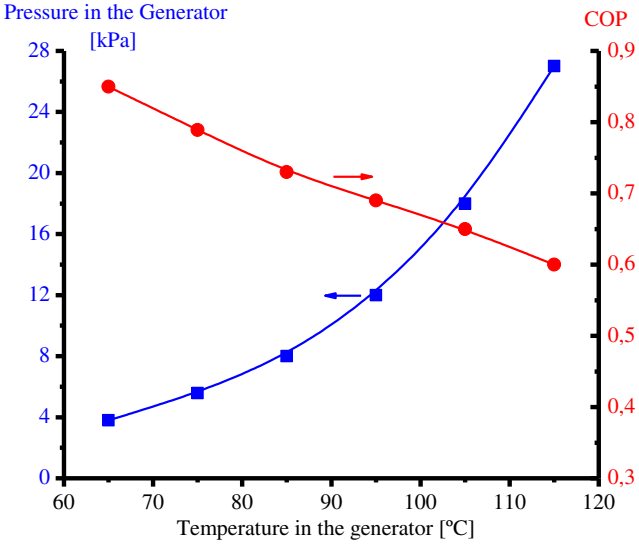

Fig. C2 – Influence of the generator outlet temperature on the coefficient of performance and absorber exit temperature (cooling capacity of 10 kW).

REFERENCES

Al-Otaibi, D.A., Dincer, I., Kalyon, M., 2004. Thermoeconomic optimization of vapor-compression refrigeration systems. Int. Comm. Heat Mass Transf. 31 (1), 95–107.

Arora, A., Kaushik, S.C., 2009. Theoretical analysis of LiBr/H_2O absorption refrigeration systems. Int. J. Energ. Res. 33 (15), 1321–1340.

Barton, P.I., Pantelides, C.C., 1993. gPROMS – a combined discrete/continuous modeling environment for chemical processing systems. Sim. Ser. 25 (3), 25–34.

Biegler, L.T., Grossmann, I.E., Westerberg, A.W., 1997. Systematic Methods of Chemical Process Design. Prentice Hall.

Brooke, A., Kendrick, D., Meeraus, A., 1996. GAMS – a User's Guide (Release 2.25). The Scientific Press, San Francisco, CA.

Castro, J., Oliva, A., Perez-Segarra, C.D., Oliet, C., 2008. Modelling of the heat exchangers of a small capacity, hot water driven, air-cooled H_2O–LiBr absorption cooling machine. Int. J. Refrigeration 31 (1), 75–86.

Chávez-Islas, L.M., Heard, C.L., 2009. Optimization of a simple ammonia-water absorption refrigeration cycle by application of mixed-integer nonlinear programming. Ind. Eng. Chem. Res. 48 (4), 1957–1972.

Chávez-Islas, L.M., Heard, C.L., Grossmann, I.E., 2009. Synthesis and optimization of an ammonia/water absorption refrigeration cycle considering different types of heat exchangers by application of mixed-integer nonlinear programming. Ind. Eng. Chem. Res. 48 (6), 2972–2990.

Drud, A.S., 1992. CONOPT, a GRG Code for Large Scale Non Linear Optimization. Reference manual. ARKI Consulting and Development A/S, Bagsvaerd, Denmark.

Feng, X., Zhu, X.X., 1997. Combining pinch and exergy analysis for modification processes. Appl. Therm. Eng. 3, 249–261.

Florides, G.A., Kalogirou, S.A., Kalogirou, S.A., Tassou, S.A., Wrobel, L.C., 2003. Design and construction of a LiBr-water absorption machine. Energ. Convers. Manage. 44, 2483–2508.

Floudas, C.A., 2000. Deterministic Global Optimization: Theory, Methods and Applications. In: Nonconvex Optimization and Its Applications. Kluwer Academic Publishers, Dordrecht, Netherlands.

Fourer, R.., Gay, D.M., Kernighan, B.W., 1990. A modelling language for mathematical programming. Manage. Sci. 36, 519–554.

Gebreslassie, B.H., Guillén-Gosálbez, G., Jiménez, L., Boer, D., 2009a. Design of environmentally conscious absorption cooling systems via multi-objective optimization and life cycle assessment. Appl. Energ. 86 (9), 1712–1722.

Gebreslassie, B.H., Guillén-Gosálbez, G., Jiménez, L., Boer, D., 2009b. Economic performance optimization of an absorption cooling system under uncertainty. Appl. Therm. Eng. 29 (17–18), 3491–3500.

Gebreslassie, B.H., Medrano, M., Mendes, F., Boer, D., 2010. Optimum heat exchanger area estimation using coefficients of structural bonds: application to an absorption chiller. Int. J. Refrigeration 33 (3), 529–537.

Gebreslassie, B.H., Groll, E.A., Garimella, S.V., 2012. Multi-objective optimization of sustainable single-effect Water/Lithium bromide absorption cycle. Renew. Energ. 46, 100–110.

Godarzi, A.A., Jalilian, M., Samimi, J., Jokar, A., Vesaghi, M.A., 2013. Design of a PCM storage system for a solar absorption chiller based on exergoeconomic analysis and genetic algorithm. Int. J. Refrigeration 36 (1), 88–101.

Goedkoop, M., Spriensma, R., 2000. The Eco-indicator 99: a Damage Oriented Method for Life Cycle Assessment. Methodology Report, second ed. Pré Consultants, Amersfoort (NL), Netherlands.

Grossman, G., Lando, J.L., Vardi, I., Bourne, J.R., Kimchi, Y., Ben-Dror, J., May 1979. Solar powered environment control criteria and realization. In: Boer, K.W., Glenn, B.H. (Eds.), Proceedings, the 1979 International Solar Energy Society Conference, vol. 1. Pergamon Press, Atlanta, Ga, pp. 720–724.

Grossman, G., 1982. Adiabatic Absorption and Desorption for Improvement of Temperature-boosting Adsorption Heat Pumps. ORNL/TM-8390. Oak Ridge National Laboratory.

Grossman, G., Childs, K.W., 1983. Computer simulation of a lithium bromide-water absorption heat pump for temperature boosting. ASHRAE Trans. 89 (1b), 240–248.

Grossman, G., 1998. Modular Simulation of Absorption Systems. User's Guide and Reference Windows. Version 5.0 (AbsimW). Oak Ridge National Laboratory. ORNL/Sub/86-XSY123V http://www.ornl.gov/~webworks/cpr/rpt/107911.pdf.

Grossmann, I.E., 2002. Review of non linear mixed-integer and disjunctive programming techniques. Optim. Eng. 3, 227–252.

Kaynakli, O., Yamankaradeniz, R., 2007. Thermodynamic analysis of absorption refrigeration system based on entropy generation. Curr. Sci. 92 (4), 472–479.

Kızılkan, Ö., Şencan, A., Kalogirou, S.A., 2007. Thermoeconomic optimization of a LiBr absorption refrigeration system. Chem. Eng. Process. 46 (12), 1376–1384.

Kodal, A., Sahin, B., Oktem, A.S., 2000. Performance analysis of two stage combined heat pump system based on termoeconomic optimization criterion. Energ. Convers. Manage. 41 (18), 1989–2008.

Kodal, A., Sahin, B., Erdil, A., 2002. Performance analysis of a two-stage irreversible heat pump under maximum heating load per unit total cost conditions. Int. J. Exergy 2 (3), 159–166.

Kodal, A., Sahin, B., Ekmekei, I., Yilmaz, T., 2003. Thermoeconomic optimization for irreversible absorption refrigeratos and heat pumps. Energ. Convers. Manage. 44 (1), 109–123.

Marcos, J.D., Izquierdo, M., Palacios, E., 2011. New method for COP optimization in water- and air-cooled single and double effect LiBr-water absorption machines. Int. J. Refrigeration 34 (6), 1348–1359.

McLinden, M.O., Klein, S.A., 1985. Steady state modeling of absorption heat pumps with a comparison to experiments. ASHRAE Trans. 91 (2b), 1793–1807.

Misra, R.D., Sahoo, P.K., Sahoo, S., Gupta, A., 2003. Thermoeconomic optimization of a single effect water/LiBr vapour absorption refrigeration system. Int. J. Refrigeration 26 (2), 158–169.

Misra, R.D., Sahoo, P.K., Sahoo, S., Gupta, A., 2005. Thermoeconomic evaluation and optimization of a double-effect H_2O/LiBr vapour-absorption refrigeration system. Int. J. Refrigeration 28 (3), 331–343.

Misra, R.D., Sahoo, P.K., Sahoo, S., Gupta, A., 2006. Thermoeconomic evaluation and optimization of an aqua-ammonia vapour absorption refrigeration system. Int. J. Refrigeration 29 (1), 47–59.

Morosuk, T., Tsatsaronis, G., 2008. A new approach to the exergy analysis of absorption refrigeration machines. Energ. J. 33 (6), 890–907.

Palacios Bereche, R., Gonzales Palomino, R., Nebra, S.A., 2009. Thermoeconomic analysis of a single and double-effect LiBr/H_2O absorption refrigeration system. Int. J. Therm. 12 (2), 89–98.

Perez-Blanco, H., Patterson, M.R., 1986. Conceptual Design and Optimization of a Versatile Absorption Heat Transformer. ORNL/TM-9841. Oak Ridge National Laboratory.

Pieragostini, C., Mussati, M., Aguirre, P., 2012. On process optimization considering LCA methodology. J. Environ. Manage. 96 (1), 43–54.

Ryoo, H.S., Sahinidis, N.V., 1995. Global optimization of nonconvex MINLP problems in process synthesis. Comp. Chem. Eng. 19 (5), 551–566.

Sahin, B., Kodal, A., 2002. Thermoeconomic optimization of a two stage combined refrigeration system: a finite-time approach. Int. J. Refrigeration 25 (7), 872–877.

Sahoo, P.K., Misra, R.D., Gupta, A., 2005. Exergoeconomic optimisation of an aqua-ammonia absorption refrigeration system. Int. J. Exergy 1 (1), 82–93.

Sayyaadi, H., Nejatolahi, M., 2011. Multi-objective optimization of a cooling tower assisted vapor compression refrigeration system. Int. J. Refrigeration 34 (1), 243–256.

Sencan, A., Yakut, K.A., Kalogirou, S.A., 2005. Exergy analysis of lithium bromide/water absorption systems. Renew. Energ 30, 645–657.

Varani, C.M.R., Santos, C.A.C., Gondim, R.R., Torres, E.A., 2003. Energetic and exergetic evaluation of an lithium Bromide/Water absorption refrigeration system utilizing natural gas. In: Proc. of ECOS2003, Copenhagen, Denmark, June 30–July 2, pp. 1597–1619.

Vliet, G.C., Lawson, M.B., Lithgow, R.A., 1982. Water-lithium bromide double effect absorption cooling cycle analysis. ASHRAE Trans. 88 (1), 811–823.